# Phosphine-Based Platinum(II) Hydroxo and Oxo Complexes[1]

**Jian Jun Li, Wei Li, and Paul R. Sharp***

Department of Chemistry, University of Missouri−Columbia, Columbia, Missouri 65211

*Received May 16, 1995*[⊗]

The platinum(II) hydroxo complexes, $[L_2Pt(\mu\text{-}OH)]_2(BF_4)_2$ (**1**), have been prepared from the reaction of $L_2PtCl_2$ with $AgBF_4$ for $L_2$ = dppm, dppp, dppb, $2PMe_2Ph$, and $Bu^t_2bpy$ (dppm = bis(diphenylphosphino)methane, dppe = bis(diphenylphosphino)ethane, dppp = bis(diphenylphosphino)propane, dppb = bis(diphenylphosphino)butane, $Bu^t_2bpy$ = 4,4′-di-*tert*-butyl-2,2′-bipyridine). The trifluoroacetate ($L_2$ = dppp) and the nitrate ($L_2$ = $Bu^t_2bpy$) salts were also prepared. Two of these new hydroxo complexes, as well as the previously known $PPh_3$ complex, were structurally characterized. Crystals of $[(PPh_3)_2Pt(\mu\text{-}OH)]_2(BF_4)_2$ from $CH_2Cl_2$/ether are monoclinic (*C*2/*m*) with $a$ = 17.183(5) Å, $b$ = 18.243(4) Å, $c$ = 13.539(4) Å, $\beta$ = 130.66(2)°, and $Z$ = 2. Crystals of $[(dppm)Pt(\mu\text{-}OH)]_2(BF_4)_2\cdot 2DMF$ from DMF/$Et_2O$ are monoclinic ($P2_1/n$) with $a$ = 17.193(6) Å, $b$ = 9.341(5) Å, $c$ = 18.666(7) Å, $\beta$ = 98.73(2)°, and $Z$ = 2. Crystals of $[(dppb)Pt(\mu\text{-}OH)]_2(BF_4)_2\cdot 4MeOH$ from MeOH/$Et_2O$ are triclinic ($P\bar{1}$) with $a$ = 12.547(13) Å, $b$ = 12.858(14) Å, $c$ = 13.039(20) Å, $\alpha$ = 62.89(11)°, $\beta$ = 63.05(11)°, $\gamma$ = 60.87(12)°, and $Z$ = 1. The structures of the binuclear dications are all similar, having planar $P_2Pt(\mu\text{-}OH)_2PtP_2$ cores with pseudo-$D_{2h}$ symmetry. For all but the dppm complex, addition of 2 equiv of $LiN(SiMe_3)_2$ results in deprotonation of the hydroxo groups and formation of the oxo complexes $[L_2Pt(\mu\text{-}O)]_2$. The isolated oxo complexes are associated with one (L = $PPh_3$) or two (L = $PMe_2Ph$; $L_2$ = dppe, dppp, dppb, $Bu^t_2bpy$) LiX units (X = $BF_4$ or $CF_3CO_2$) by interaction of the oxo ligands with the Li cations. The structure of $[(PPh_3)_2Pt(\mu\text{-}O)]_2\cdot LiBF_4$ (**2**) was determined. Crystals of $\mathbf{2}\cdot 0.5C_7H_8$ from toluene are monoclinic (*C*2/*c*), with (173 K) $a$ = 20.469(8) Å, $b$ = 18.085(9) Å, $c$ = 18.152(8) Å, $\beta$ = 90.34(6)°, and $Z$ = 4. The structure consists of two edge-shared square planar Pt atoms folded at the edge with cis-phosphines and bridging oxygen atoms. The bridging oxo oxygen atoms are coordinated to the Li cation of a $LiBF_4$ contact ion pair. Two fluorine atoms of the $BF_4$ ion also coordinate to the Li cation, resulting in a flattened tetrahedral environment about the Li cation. The oxo complex $[(PMe_2Ph)_2Pt(\mu\text{-}O)]_2\cdot(LiBF_4)_2$ is unstable in solution and converts to the $\mu_3$-oxo complex $[(L_2Pt)_3(\mu_3\text{-}O)_2](BF_4)_2$ (**5**) (L = $PMe_2Ph$). Crystals of **5** from THF are orthorhombic (*Pbna*), with (173 K) $a$ = 16.792(4) Å, $b$ = 17.710(5) Å, $c$ = 19.648(6) Å, and $Z$ = 4. The core structure of the dication consists of a dioxo-bicapped $Pt_3$ triangle. Deprotonation of the dppm hydroxo complex **1** ($L_2$ = dppm) occurs at the dppm methylene group and not at the hydroxo group. The resulting neutral hydroxo complex $[(dppm\text{-}H)Pt(\mu\text{-}OH)]_2$ (**6**) (dppm-H = bis(diphenylphosphino)methanide) is further deprotonated in THF at the OH group, giving the structurally characterized anionic oxo complex $[(dppm\text{-}H)Pt(\mu\text{-}O)]_2[Li(THF)_2]_2$ (**7**). Crystals of $\mathbf{7}\cdot 4THF$ from THF are monoclinic ($P2_1/c$), with (173 K) $a$ = 10.534(2) Å, $b$ = 21.016(2) Å, $c$ = 18.402(4) Å, $\beta$ = 103.41(1)°, and $Z$ = 2. The structure has a planar core with the deprotonation of the dppm ligand evident from a shortening of the P−C distances. The Li ions are associated with the oxo groups, not the dppm-H groups, and are each coordinated by two THF molecules, giving a trigonal planar Li coordination geometry.

## Introduction

Many interesting and important reactions are catalyzed by late transition metal surfaces. Surface-bound oxygen and nitrogen species are usually involved in these reactions.[2] We have been studying late transition metal oxo and imido complexes in order to test the possibility of bringing some of this surface chemistry into solution and have reported investigations into the oxo and imido chemistry of Rh and Ir[3] and Au.[4] Our success with Rh and Ir oxo chemistry was due to the availability of cationic hydroxo complexes that could be deprotonated to the oxo complexes. The large number of known Pt hydroxo complexes and the importance of Pt in catalytic chemistry inspired us to explore the synthesis of Pt oxo complexes. Interest in the area of Pt hydroxo chemistry has been partly driven by the antitumor activity of *cis*-$(NH_3)_2PtCl_2$ (*cis*-platin) and related complexes where hydrolysis is an important step in the activity of the drug.[5] In this paper we focus on Pt(II) hydroxo complexes with phosphine ligands and one example with a bipyridine ligand. We find that deprotonation of the hydroxo complexes is successful and produces a series of dimeric dioxo complexes of Pt(II). In addition to the preparation and characterization of these dioxo complexes, we

[⊗] Abstract published in *Advance ACS Abstracts,* December 15, 1995.

(1) Part 16.: Late Transition Metal Oxo and Imido Complexes. Part 15: Ye, C.; Sharp, P. R. *Inorg. Chem.* **1995**, *34*, 55−59.

(2) (a) Madix, R. J.; Jorgensen, S. W. *Surf. Sci.* **1987**, *183*, 27. (b) Akhter, S.; White, J. M. *Surf. Sci.* **1986**, *167*, 101. (c) Berlowitz, P.; Yang, B. L.; Butt, J. B.; Kung, H. H. *Surf. Sci.* **1986**, *171*, 69. (d) Outka, D. A.; Madix, R. J. *J. Am. Chem. Soc.* **1987**, *109*, 1708. (e) Lueng, L.-W. H.; Weaver, M. J. *J. Am. Chem. Soc.* **1987**, *109*, 5113. (f) Roberts, J. T.; Madix, R. J. *J. Am. Chem. Soc.* **1988**, *110*, 8540. (g) Friend, C. M.; Xu, X. *J. Am. Chem. Soc.* **1990**, *112*, 4571.

(3) (a) Sharp, P. R.; Flynn, J. R. *Inorg. Chem.* **1987**, *26*, 3231−3234. (b) Ge, Y.-W.; Peng, F.; Sharp, P. R. *J. Am. Chem. Soc.* **1990**, *112*, 2632−2640. (c) Ge, Y.-W.; Sharp, P. R. *Inorg. Chem.* **1992**, *31*, 379−384. (d) Ge, Y.-W.; Sharp, P. R. *Inorg. Chem.* **1993**, *32*, 94−100. (e) Ge, Y.-W.; Ye, Y.; Sharp, P. R. *J. Am. Chem. Soc.* **1994**, *116*, 8384−8385. (f) Ye, C.; Sharp, P. R. *Inorg. Chem.* **1995**, *34*, 55−59.

(4) (a) Ramamoorthy, V.; Sharp, P. R. *Inorg. Chem.* **1990**, *29*, 3336−3338. (b) Ramamoorthy, V.; Wu, Z.; Yi, Y.; Sharp, P. R. *J. Am. Chem. Soc.* **1992**, *114*, 1526−1527. (c) Yang, Y.; Sharp, P. R. *Inorg. Chem.* **1993**, *32*, 1946−1951. (d) Yang, Y.; Wu, Z.; Ramamoorthy, V.; Sharp, P. R. in *The Chemistry of the Copper and Zinc Triads*; Welch, A. J., Chapman, S. K., Eds.; The Royal Society of Chemistry: Cambridge, 1993. (e) Yang, Y.; Sharp, P. R. *J. Am. Chem. Soc.* **1994**, *116*, 6983−6984.

(5) Sherman, S. E.; Lippard, S. J. *J. Chem. Soc.* **1987**, *87*, 1153−1181.

0020-1669/96/1335-0604$12.00/0 

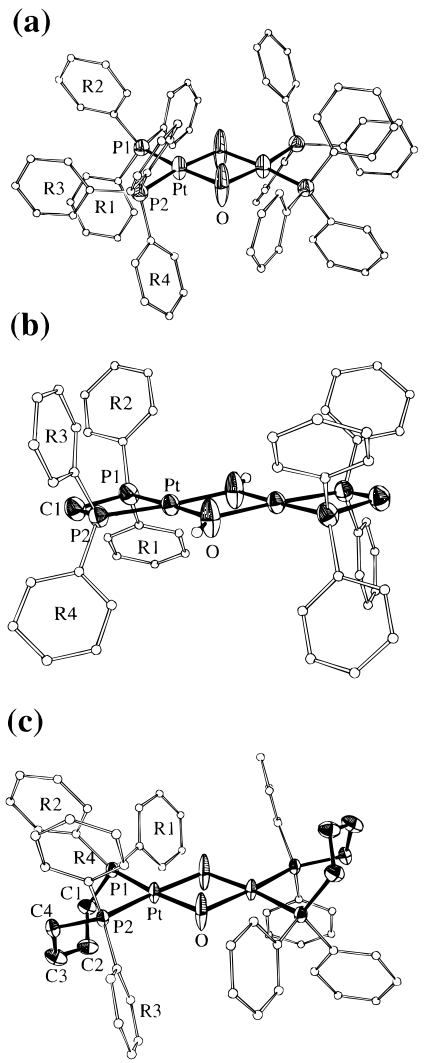


**Figure 1.** ORTEP drawings of the cationic portions of $[L_2Pt(\mu\text{-}OH)]_2(BF_4)_2$ (**1**): (a) L = $PPh_3$; (b) L = dppm; (c) L = dppb.

also report the synthesis of some new hydroxo complexes and the structures of three of the hydroxo complexes. Portions of this work have been previously communicated.[6]

## Results

**Hydroxo Complexes**. The hydroxo complexes $[L_2Pt(\mu\text{-}OH)]_2(BF_4)_2$ (**1**) ($L_2$ = dppm, dppe, dppp, dppb, $2PMe_2Ph$, $Bu^t_2$bpy)[7] are readily prepared by treating $L_2PtCl_2$[8] with $AgBF_4$ (eq 1). Analogous trifluoroacetate ($L_2$ = dppp) and nitrate ($L_2$ = $Bu^t_2$bpy) salts were similarly prepared. The preparations follow procedures previously developed for related complexes[9] but are slightly modified for each L or $L_2$. The outcomes of the reactions are sensitive to the solvent and the amount of water present in the solvent. Very low levels of water in EtOH are required for L = dppm, while 90−95% MeOH or EtOH is effective for the other phosphines and the bipyridine complex.

$$2L_2PtCl_2 + 4AgBF_4 + 2H_2O \rightarrow \underset{\mathbf{1}}{[L_2Pt(\mu\text{-}OH)]_2(BF_4)_2} + 4AgCl + 2HBF_4 \quad (1)$$

$^{31}$P NMR spectra of the phosphine-containing hydroxo complexes show the expected singlets flanked by $^{195}$Pt satellites. Unlike for the $PMe_3$ complex,[10] no third order P−Pt coupling is observed. The shifts for the bidentate phosphine complexes are consistent with chelation of the phosphine ligands.[11] $^1$H NMR spectra show, in addition to signals for the phosphine or bpy ligand peaks, OH group singlets that range from 6.50 to 1.32 ppm. The OH peaks for the dppm, $PMe_2Ph$, and $Bu^t_2$bpy complexes appear at the upper end of this range. IR spectra show weak OH bands at ca. 3500 $cm^{-1}$ similar to those previously reported for the $PPh_3$ and $PEt_3$ hydroxo complexes.[9] An exception is the dppm complex for which the band appears at 3200 $cm^{-1}$, 300 $cm^{-1}$ lower than those of the other complexes.

The solid state structures of three of the hydroxo complexes **1** (L = $PPh_3$; $L_2$ = dppm, dppb) were determined by X-ray crystallography. ORTEP diagrams are shown in Figure 1. An abbreviated summary of crystal data and data collection and processing is given in Table 1. Selected atomic coordinates are given in Table 2, and selected bond distances and angles are listed in Table 3. All three of the structures show planar pseudo-$D_{2h}$-symmetric $P_2Pt(\mu\text{-}O)_2PtP_2$ units with crystallographic inversion (dppb and dppm) or 2-fold/mirror symmetry ($PPh_3$).

**Oxo Complexes. L = $PPh_3$.** Addition of excess (∼4 equiv)[12] $LiN(SiMe_3)_2$ to white suspensions of $[(PPh_3)_2Pt(\mu\text{-}OH)]_2(BF_4)_2$ in THF gives homogeneous pale yellow solutions. $^{31}$P NMR spectra of the solutions show a single peak with $^{195}$Pt satellites indicating the formation of a single Pt−P-containing product. The coupling constant (3286 Hz) is reduced by almost 500 Hz from that of the hydroxo precursor. Removal of the volatiles leaves a residue which dissolves in toluene or $Et_2O$ and again shows a single peak with satellites and the same coupling constant. With time, white crystals precipitate from the $Et_2O$ or toluene solutions. Once deposited, the crystals are insoluble in toluene and $Et_2O$, slightly soluble in THF, and soluble in methylene chloride. $^{31}$P NMR spectra of the dissolved crystals in $CH_2Cl_2$ again show a single peak with the same Pt−P coupling constant as in the previous solutions. $^{19}$F NMR and IR spectroscopies of the isolated crystals indicate the presence of $BF_4$. This is confirmed by an X-ray crystal structure determination and indicates the final reaction stoichiometry of eq 2 (R = $SiMe_3$).

$$\underset{\mathbf{1}\ (L = PPh_3)}{[(PPh_3)_2Pt(\mu\text{-}OH)]_2(BF_4)_2} + 2LiNR_2 \rightarrow \underset{\mathbf{2}}{[(PPh_3)_2Pt(\mu\text{-}O)]_2\cdot LiBF_4} + LiBF_4 + 2HNR_2 \quad (2)$$

An ORTEP view of the structure is given in Figure 2 and shows a Pt oxo-bridged dimer consisting of two edge-shared square planar Pt centers folded at the shared edge. The bridging oxo groups are coordinated to a Li cation of a $LiBF_4$ contact ion pair. Two fluorine atoms of the tetrafluoroborate anion also interact closely with the Li cation, resulting in a flattened

(6) ) (a) Li, J. J.; Sharp, P. R. *Inorg. Chem.* **1994**, *33*, 183−184. (b) Li, W.; Barnes, C. L.; Sharp, P. R. *J. Chem. Soc., Chem. Commun.* **1990**, 1634−1636.

(7) Abbreviations: dppm = bis(diphenylphosphino)methane, dppe = bis(diphenylphosphino)ethane, dppp = bis(diphenylphosphino)propane, dppb = bis(diphenylphosphino)butane, dppm-H = bis(diphenylphosphino)methanide, $Bu^t_2$bpy = 4,4′-di-*tert*-butyl-2,2′-bipyridine.

(8) Brown, M. P.; Puddephatt, R. J.; Rashidi, M.; Seddon, K. R. *J. Chem. Soc., Dalton Trans.* **1977**, 951.

(9) (a) Bushnell, G. W.; Dixon, K. R.; Hunter, R. G.; McFarland, J. J. *Can. J. Chem.* **1972**, *50*, 3694. (b) Wimmer, S.; Castan, P.; Wimmer, F. L.; Johnson, N. P. *J. Chem. Soc., Dalton Trans.* **1989**, 403−412.

(10) Trovó, G.; Bandoli, G.; Casellato, U.; Corain, B.; Nicolini, M.; Longato, B. *Inorg. Chem.* **1990**, *29*, 4616−4621.

(11) Garrou, P. E. *Chem. Rev.* **1981**, *81*, 229−266.

(12) If excess $LiN(SiMe_3)_2$ is not used, large amounts of an insoluble pale yellow material are produced. A weak OH band in the IR spectrum suggests that this is the single deprotonation product $[(L_2Pt)_2(\mu\text{-}OH)(\mu\text{-}O)](BF_4)$.

**Table 1.** Crystallographic and Data Collection Parameters

| | **1** (L = $PPh_3$) | **1** ($L_2$ = dppm)·2DMF | **1** ($L_2$ = dppb) | **2** | **5** | **7** |
|---|---|---|---|---|---|---|
| formula | $C_{72}H_{62}O_2P_4Pt_2$ $2(BF_4)$ | $Pt_2C_{50}H_{46}O_2P_4$ $2(BF_4)\cdot 2C_3H_7NO$ | $Pt_2C_{56}H_{58}O_2P_4$ $2(BF_4)\cdot 4CH_3OH$ | $Pt_2C_{72}H_{60}O_2P_4\cdot$ $LiBF_4\cdot 0.5C_7H_8$ | $Pt_3C_{48}H_{66}O_2P_6$ $2(BF_4)$ | $Pt_2C_{50}H_{42}O_2P_4Li_2\cdot$ $8C_4H_8O$ |
| fw | 1646.98 | 1512.80 | 1578.94 | 1611.2 | 1619.78 | 1779.71 |
| space group | *C*2/*m* (no. 12) | $P2_1/n$ (no. 14) | $P\bar{1}$ (no. 2) | *C*2/*c* (no. 15) | *Pbna* (no. 60) | $P2_1/c$ (no. 14) |
| *T*, °C | 22 | 22 | −100 | −100 | 22 | −100 |
| *a*, Å | 17.183(5) | 17.193(6) | 12.547(13) | 20.469(8) | 16.792(4) | 10.534(2) |
| *b*, Å | 18.243(4) | 9.341(5) | 12.858(14) | 18.085(9) | 17.710(5) | 21.016(2) |
| *c*, Å | 13.539(4) | 18.666(7) | 13.039(20) | 18.152(8) | 19.648(6) | 18.402(4) |
| α, deg | | | 62.89(11) | | | |
| *β*, deg | 130.66(2) | 98.73(2) | 63.05(11) | 90.34(6) | | 103.41(1) |
| *γ*, deg | | | 60.87(12) | | | |
| *V*, $Å^3$ | 3219(2) | 2963(2) | 1562(3) | 6719(2) | 5843(3) | 3963(1) |
| *Z* | 2 | 2 | 1 | 4 | 4 | 2 |
| $d_{calc}$, $g/cm^3$ | 1.70 | 1.70 | 1.68 | 1.59 | 1.84 | 1.49 |
| *λ*, Å | 0.7093 (Mo) | 0.7093 (Mo) | 0.7093 (Mo) | 0.7107 (Mo) | 0.7093 (Mo) | 1.5406 (Cu) |
| *μ*, $mm^{-1}$ | 4.64 | 4.93 | 9.35 | 4.35 | 4.97 | 15.6 |
| transm range, % | 82.6−100 | 6.54−100 | 72.9−99.7 | 82.0−100 | 74.3−100 | 67.7−99.8 |
| $R(F_0)$,[a] $R_w(F_0)$[b] | 0.051, 0.068 | 0.023, 0.034 | 0.025, 0.030 | 0.048, 0.070 | 0.039, 0.057 | 0.058, 0.071 |

[a] $R(F_o) = (\sum||F_o| - |F_c||)/\sum F_o$. [b] $R_w(F_o) = [(\sum w(|F_o| - |F_c|)^2)/\sum wF_o^2]^{1/2}$; $w = 4F_o^2/(\sum F_o^2)^2$.

**Table 2.** Selected Atomic Parameters

| | *x* | *y* | *z* | *B*(iso)[a] |
|---|---|---|---|---|
| | | $[L_2Pt(\mu\text{-OH})]_2(BF_4)_2$ (**1**) (L = $PPh_3$) | | |
| Pt | 0.08187(4) | 0 | 0.15341(5) | 4.39(5) |
| O1 | 0.0757(8) | 0 | −0.0032(11) | 10.8(13) |
| P1 | 0.2511(3) | 0 | 0.2922(3) | 3.21(23) |
| P2 | 0.0561(3) | 0 | 0.2952(3) | 3.25(23) |
| | | $[L_2Pt(\mu\text{-OH})]_2(BF_4)_2$ (**1**) ($L_2$ = dppm) | | |
| Pt | 0.01862(1) | 0.92882(2) | 0.080814(9) | 2.85(1) |
| P1 | −0.02480(8) | 0.90321(16) | 0.18603(7) | 3.32(6) |
| P2 | 0.10347(7) | 0.78674(15) | 0.14757(7) | 3.09(5) |
| O | −0.0635(3) | 1.0482(5) | 0.0143(2) | 5.4(2) |
| C1 | 0.0582(3) | 0.7963(7) | 0.2304(3) | 4.0(3) |
| HO | −0.099(4) | 1.080(7) | 0.021(4) | 6.3 |
| | | $[L_2Pt(\mu\text{-OH})]_2(BF_4)_2$ (**1**) ($L_2$ = dppb) | | |
| Pt | 0.41321(1) | 0.42030(1) | 0.04074(1) | 2.46(1) |
| P1 | 0.42144(10) | 0.22596(9) | 0.15183(9) | 1.95(5) |
| P2 | 0.22903(9) | 0.47217(9) | 0.01405(9) | 1.94(5) |
| O | 0.5778(4) | 0.4022(3) | 0.0597(5) | 6.1(3) |
| | | $[L_2Pt(\mu\text{-O})]LiBF_4$ (L = $PPh_3$) (**2**)[b] | | |
| Pt | 0.42752(2) | 0.28860(2) | 0.24670(3) | 0.024 |
| P1 | 0.3590(1) | 0.2760(1) | 0.1507(2) | 0.025 |
| P2 | 0.3607(1) | 0.2668(2) | 0.3431(2) | 0.027 |
| O | 0.4985(3) | 0.3189(4) | 0.3199(3) | 0.027 |
| F1 | 0.5351(6) | 0.4955(5) | 0.2944(6) | 0.124 |
| F2 | 0.4599(13) | 0.5848(8) | 0.2868(9) | 0.267 |
| B | 1/2 | 0.544(1) | 1/4 | 0.112 |
| Li | 1/2 | 0.410(1) | 1/4 | 0.045 |
| | | $[(L_2Pt)_3(\mu\text{-O})_3](BF_4)_2$ (L = $PMe_3Ph$) (**5**) | | |
| Pt1 | 0.60357(4) | 1/4 | 0 | 3.21(3) |
| Pt2 | 0.75219(3) | 0.27400(3) | 0.06983(3) | 3.86(3) |
| P1 | 0.5150(2) | 0.1656(2) | 0.0362(2) | 4.2(2) |
| P2 | 0.8048(3) | 0.3833(3) | 0.1041(2) | 5.2(2) |
| P3 | 0.7918(3) | 0.2053(3) | 0.1588(2) | 5.3(2) |
| O | 0.7027(5) | 0.1825(5) | 0.0198(4) | 3.6(4) |
| | | $[L_2Pt(\mu\text{-O})]_2Li_2$ ($L_2$ = dppm-H) (**7**) | | |
| Pt | 0.54698(5) | 0.43603(2) | 0.03980(2) | 3.45(2) |
| P1 | 0.6315(3) | 0.3901(1) | 0.1494(2) | 3.8(1) |
| P2 | 0.5764(3) | 0.3323(1) | 0.0236(2) | 3.9(1) |
| C1 | 0.647(1) | 0.3147(5) | 0.1151(6) | 4.4(6) |
| O1 | 0.5255(9) | 0.5300(3) | 0.0653(4) | 4.4(4) |
| Li | 0.396(3) | 0.536(1) | 0.110(1) | 6.3(12) |

[a] *B*(iso) is the mean of the principal axes of the thermal ellipsoid. [b] Thermal parameters are expressed as *U* not *B*.

tetrahedral Li geometry. Crystal and data collection parameters for the structure are given in Table 1. Selected atom coordinates are listed in Table 2, and distances and angles are given in Table 4.

**Table 3.** Distances (Å) and Angles (deg) for $[L_2Pt(\mu\text{-OH})]_2(BF_4)_2$ (**1**)

| | L = $PPh_3$ | $L_2$ = dppm | $L_2$ = dppb |
|---|---|---|---|
| Pt−O | 2.053(11) | 2.061(4) | 2.079(4) |
| Pt−Oa | 2.072(11) | 2.051(4) | 2.081(5) |
| Pt−P1 | 2.206(4) | 2.217(2) | 2.222(4) |
| Pt−P2 | 2.234(4) | 2.212(1) | 2.219(3) |
| O···O | 2.659(22) | 2.492(8) | 2.641(9) |
| Pt···Pt | 3.153(2) | 3.270(1) | 3.215(4) |
| O−Pt−Oa | 80.3(4) | 74.63(16) | 78.75(20) |
| O−Pt−P1 | 91.8(3) | 107.49(12) | 95.45(17) |
| O−Pt−P2 | 169.1(3) | 175.81(16) | 170.83(12) |
| Oa−Pt−P1 | 172.1(3) | 177.61(14) | 174.21(10) |
| Oa−Pt−P2 | 88.8(3) | 104.34(12) | 92.74(17) |
| P1−Pt−P2 | 99.08(14) | 73.63(5) | 93.04(15) |
| Pt−O−Pta | 99.7(5) | 105.37(18) | 101.25(21) |

Other deprotonating agents may be used in place of $LiN(SiMe_3)_2$ but not as effectively. The reaction of $[L_2Pt(\mu\text{-OH})]_2(BF_4)_2$ (L = $PPh_3$) with 2 equiv of $LiNPr^i_2$ in THF gives a pale-orange solution. $^{31}P$ NMR spectroscopy indicates an 80% yield of **2** and the formation of $Ph_3PO$. $Ph_3PO$ is the major product when $LiBu^n$ or LiPh are used. Substitution of $NaN(SiMe_3)_2$ for $LiN(SiMe_3)_2$ gives product **3** with no evidence for the presence of $BF_4$. Complex **3** is formulated as the salt-free analog of **2** (eq 3, R = $SiMe_3$). $^{31}P$ NMR spectra of **3** again show a single peak flanked by $^{195}Pt$ satellites with a coupling constant (3180 Hz) that is ca. 100 Hz smaller than that of the $LiBF_4$ adduct **2**.

$$[(PPh_3)_2Pt(\mu\text{-OH})]_2(BF_4)_2 + 2NaNR_2 \rightarrow \underset{\textbf{1}\ (L = PPh_2)}{} \qquad [(PPh_3)_2Pt(\mu\text{-O})]_2 + 2NaBF_4 + 2HNR_2 \quad (3)$$
$$\textbf{3}$$

**$L_2$ = dppe, dppp, dppb, $Bu^t_2$bpy.** Deprotonation of the $L_2$ = dppe, dppp, dppp, and $Bu^t_2$bpy hydroxo complexes $[L_2Pt(\mu\text{-OH})]_2(BF_4)_2$ (**1**) all proceed similarly. Addition of $LiN(SiMe_3)_2$ to THF suspensions of the hydroxo complexes gives yellow or red ($Bu^t_2$bpy) homogeneous solutions. $^{31}P$ NMR spectra of the reaction mixtures of the phosphine complexes show in each case a single product with Pt−P coupling constants reduced from those of the hydroxo precursors and with shifts consistent with retention of phosphine chelation. $^1H$ NMR spectra of all of the complexes show signals for the phosphine or bpy ligand and the loss of the OH peaks. The reaction of the dppe complex is more sensitive than the others and

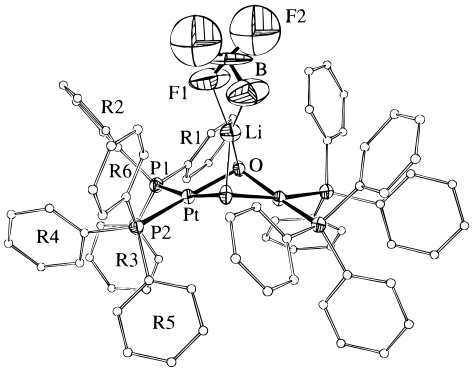


**Figure 2.** ORTEP drawing of $[(PPh_3)_2Pt(\mu\text{-}O)]_2{\cdot}LiBF_4$ (**2**).

**Table 4.** Distances (Å) and Angles (deg) for Oxo Complexes $[L_2Pt(\mu\text{-}O)]LiBF_4$ (L = $PPh_3$) (**2**), $[(L_2Pt)_3(\mu\text{-}O)_3](BF_4)_2$ (L = $PMe_3Ph$) (**5**), and $[L_2Pt(\mu\text{-}O)]_2Li_2$ ($L_2$ = dppm-H) (**7**)

| **2** | | **7** | | **5** | |
|---|---|---|---|---|---|
| Pt−P1 | 2.242(3) | Pt−P1 | 2.227(3) | Pt1−P1 | 2.225(4) |
| Pt−P2 | 2.262(3) | Pt−P2 | 2.232(3) | Pt2−P2 | 2.233(4) |
| Pt−O | 2.038(6) | Pt−O1 | 2.054(7) | Pt2−P3 | 2.232(4) |
| Pt−O′ | 2.018(6) | Pt−O1′ | 2.036(7) | Pt1−O | 2.086(8) |
| Li−O | 2.08(2) | Li−O1 | 1.76(2) | Pt2−O | 2.069(8) |
| F1−Li | 1.89(2) | Li−O2 | 1.92(3) | Pt2−O′ | 2.093(8) |
| F1−B | 1.38(2) | Li−O3 | 1.94(3) | Pt1−Pt2 | 2.879(1) |
| F2−B | 1.30(2) | P1−C1 | 1.73(1) | Pt2−Pt2′ | 2.873(1) |
| Pt−Pt′ | 2.969(1) | P2−C1 | 1.72(1) | | |
| | | C1−H1 | 1.1(1) | | |
| | | Pt−Pt′ | 3.112(1) | | |
| P1−Pt−P2 | 101.9(1) | P1−Pt−P2 | 70.08(10) | Pt−Pt1−P1′ | 96.12(14) |
| P1−Pt−O | 166.9(2) | P1−Pt−O1 | 104.57(21) | P1−Pt1−O | 95.1(3) |
| P1−Pt−O′ | 91.7(2) | P1−Pt−O1′ | 174.32(20) | P1−Pt1−O′ | 167.91(24) |
| P2−Pt−O | 88.6(2) | P2−Pt−O1 | 174.64(21) | O−Pt1−O′ | 74.1(3) |
| P2−Pt−O′ | 165.8(2) | P2−Pt−O1′ | 104.40(21) | P2−Pt2−P3 | 96.82(17) |
| O−Pt−O′ | 77.4(3) | O1−Pt−O1′ | 81.0(3) | P2−Pt2−O | 168.92(24) |
| Pt−O−Pt′ | 94.1(3) | Pt−O1−Pt′ | 99.0(3) | P2−Pt2−O′ | 95.3(3) |
| Pt−O−Li | 80.1(4) | Pt−O1−Li | 108.1(10) | P3−Pt2−O | 93.73(24) |
| Pt−O′−Li | 80.5(4) | Pt′−O1−Li | 105.4(9) | P3−Pt2−O′ | 167.9(3) |
| B−F1−Li | 94.1(10) | O1−Li−O2 | 128.7(14) | O−Pt2−O′ | 74.3(3) |
| O−Li−O′ | 75.3(9) | O1−Li−O3 | 119.7(17) | Pt1−O−Pt2 | 87.7(3) |
| O−Li−F1 | 113.3(4) | O2−Li−O3 | 111.4(11) | Pt1−O−Pt2′ | 87.1(3) |
| O−Li−F1′ | 154.7(4) | P1−C1−P2 | 96.0(6) | Pt2−O−Pt2′ | 87.3(3) |
| F1−Li−F1′ | 69.6(10) | P1−C1−H1 | 142(5) | | |
| | | P2−C1−H1 | 120(5) | | |

sometimes gives additional unidentified products. Consistently good results are obtained for the dppe complex by cooling the THF suspensions of the hydroxo complex to −30 °C prior to the addition of $LiN(SiMe_3)_2$.

The isolation procedure for the products is somewhat different from that of the $PPh_3$ oxo complexes. Unlike that of the $PPh_3$ complexes, THF removal leaves a toluene and $Et_2O$ insoluble solid. Therefore, the oxo complexes of these bidentate ligands are isolated by reduction of the THF solutions and precipitation with hexane or $Et_2O$. With $L_2$ = dppb, reduction of the THF solution gives crystals of the product without addition of hexane. As with the $PPh_3$ oxo complex **2**, $LiBF_4$ units are associated with the isolated complexes. NMR and elemental analysis data, however, indicate that two $LiBF_4$ units are associated with each complex yielding $[L_2Pt(\mu\text{-}O)]_2{\cdot}2LiBF_4$ (**4**) (eq 4, $L_2$ = dppe, dppp, dppb, $Bu^t_2bpy$; R = $SiMe_3$). Integration of the $^{19}F$ NMR signals for $BF_4$ against an internal standard confirms the presence of two $LiBF_4$ units. The trifluoroacetate analog of **4** ($L_2$ = dppp) was similarly prepared and characterized.

$$[L_2Pt(\mu\text{-}OH)]_2(BF_4)_2 + 2LiNR_2 \rightarrow \underset{\mathbf{1}}{} \qquad [L_2Pt(\mu\text{-}O)]_2{\cdot}2LiBF_4 + 2HNR_2 \quad (4)$$
$$\underset{\mathbf{4}}{}$$

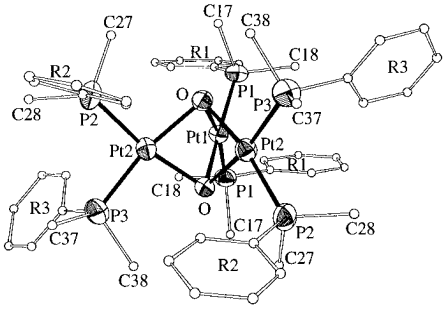


**Figure 3.** ORTEP drawing of the cationic portion of $[(L_2Pt)_3(\mu\text{-}O)_2](BF_4)_2$ (L = $PMe_2Ph$) (**5**).

**L = $PMe_2Ph$.** Deprotonation of the $PMe_2Ph$ hydroxo complex with $LiN(SiMe_3)_2$ also proceeds as in eq 4 (L = $PMe_2Ph$, X = $BF_4$). However, the resulting oxo complex $[L_2Pt(\mu\text{-}O)]_2{\cdot}2LiBF_4$ (**4**) (L = $PMe_2Ph$) is unstable in solution and must be isolated quickly from the cold reaction mixtures. The complex is stable in the solid state. Solutions decompose to a new product (**5**) in high yield (eq 5, L = $PMe_2Ph$). The $^{31}P$ NMR spectrum of **5** shows a single peak flanked by $^{195}Pt$ satellites with a P−Pt coupling constant that is much larger than that of the oxo complex **4** and is similar to that of the starting hydroxo complex. Crystals of the product form readily from THF, and an X-ray analysis reveals a trinuclear dioxo dication where two oxo groups cap a triangle formed by three $L_2Pt$ units. An ORTEP view of the dication is given in Figure 3. Crystal and data collection parameters are given in Table 1. Selected atom coordinates are listed in Table 2 while distances and angles are given in Table 4.

$$1.5[L_2Pt(\mu\text{-}O)]_2{\cdot}LiBF_4 \rightarrow [(L_2Pt)_3(\mu_3\text{-}O)_2](BF_4)_2 + \ldots \quad (5)$$
$$\mathbf{2}\ (L = PMe_2Ph) \qquad\qquad \mathbf{5}$$

**$L_2$ = dppm.** Initially, it appears that the dppm hydroxo complex is deprotonated analogously to the other phosphine complexes. The $^{31}P$ NMR signal shift confirms retention of the phosphine chelation and a decrease in the P−Pt coupling constant (from 3023 to 2830 Hz) is observed as above. However, other spectroscopic data quickly reveals features inconsistent with deprotonation of the hydroxo groups. First, unlike the above oxo complexes, the dppm deprotonation product shows no evidence of associated Li salts. Second, $^1H$ NMR spectra show, in addition to the Ph resonances, two equal intensity singlets at 3.82 and −0.41 ppm. Although we are unable to detect an OH band in the IR spectra, this data is consistent with formulation of the product as the deprotonated dppm (dppm-H) hydroxo complex **6** (eq 6, R = $SiMe_3$). $^{13}C$ NMR spectroscopy, which could confirm the formation of the PCHP group, is not possible due to the poor solubility and solution stability of **6**. However, further support of the formulation is provided by the subsequent deprotonation of the hydroxo groups of **6** with additional base.

$$[(dppm)Pt(\mu\text{-}OH)]_2(BF_4)_2 + 2LiNR_2 \rightarrow \underset{\mathbf{1}\ (L_2 = dppm)}{} \qquad [(dppm\text{-}H)Pt(\mu\text{-}OH)]_2 + 2LiBF_4 + 2HNR_2 \quad (6)$$
$$\underset{\mathbf{6}}{}$$

Treatment of a THF suspension of **6** with 2 equiv of $LiN(SiMe_3)_2$ gives a homogeneous yellow solution. Very air sensitive yellow crystalline **7** (eq 7, R = $SiMe_3$) is isolated by volume reduction and cooling of the reaction mixture. The $^{31}P$ NMR signal shift confirms retention of the phosphine chelation, and a further decrease in the P−Pt coupling constant (from 2830

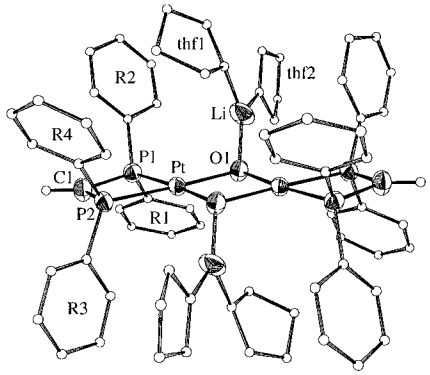


**Figure 4.** ORTEP drawing of $Li_2[(dppm\text{-}H)Pt(\mu\text{-}O)]_2\cdot 4THF$ (**7**).

to 2430 Hz) is observed. Similar results are obtained with $NaN(SiMe_3)_2$. The formulation of **7** is established by an X-ray crystal structure determination.

$$[(dppm\text{-}H)Pt(\mu\text{-}OH)]_2 + 2LiNR_2 \rightarrow \underset{\mathbf{6}}{\phantom{x}} \qquad \underset{\mathbf{7}}{Li_2[(dppm\text{-}H)Pt(\mu\text{-}O)]_2\cdot 4THF} + 2HNR_2 \quad (7)$$

An ORTEP view of **7** is shown in Figure 4. Crystal and data collection parameters are given in Table 1. Selected atom coordinates are listed in Table 2, and distances and angles are given in Table 4. The structure consists of a planar $P_2Pt(O)_2PtP_2$ array with $Li(THF)_2$ units interacting with the bridging oxo ligands above and below the planar array. As observed in other structures of dppm-H complexes,[3b,13] the deprotonated bridging carbon is planar with shortened P−C bonds. (Compare the P−C(phenyl) distances to the P−C−P distances.)

**Oxo/Hydroxo Reactions**. A measurement of the relative basicity of the oxo complexes should be possible with competition experiments as described by eq 8. Ideally, such experiments should be done with all species soluble. This is not possible here since the oxo complexes decompose in all solvents in which the hydroxo complexes are reasonably soluble. We therefore undertook these experiments in THF even though the hydroxo complexes have poor solubility in THF. This should not significantly affect the results as long as all of the hydroxo complexes have equally poor solubility in THF. A series of reactions as in eq 8 with different L and L′ were monitored by $^{31}P$ NMR spectroscopy. With the combinations $L_2$ = dppb, $L'_2$ = dppp and $L_2$ = dppe, $L'_2$ = dppp, equimolar mixtures of the oxo complexes were obtained, implying approximately equal basicity of the dppe, dppp, and dppb oxo complexes. In contrast, treatment of the L = $PMe_2Ph$ or the $L_2$ = $Bu^t_2bpy$ hydroxo complexes with the $L'_2$ = dppp oxo complex result in only the $PMe_2Ph$ or the $Bu^t_2bpy$ oxo complexes, suggesting that the dppp oxo complex is more basic than the $PMe_2Ph$ or the $Bu^t_2bpy$ oxo complexes.

$$\underset{\text{solid}}{[L_2Pt(\mu\text{-}OH)]_2(BF_4)_2} + \underset{\text{solution}}{[L'_2Pt(\mu\text{-}O)]_2\cdot(LiBF_4)_2} = \underset{\text{solid}}{[L'_2Pt(\mu\text{-}OH)]_2(BF_4)_2} + \underset{\text{solution}}{[L_2Pt(\mu\text{-}O)]_2\cdot(LiBF_4)_2} \quad (8)$$

The reactions of the dppm complexes are complicated by the deprotonation of the dppm ligand. The reaction of $[L_2Pt(\mu\text{-}O)]_2\cdot(LiBF_4)_2$ ($L_2$ = dppp) with $[L_2Pt(\mu\text{-}OH)]_2(BF_4)_2$ ($L_2$ = dppm) results in proton transfer from the dppm complex to the dppp complex, producing $[L_2Pt(\mu\text{-}OH)]_2(BF_4)_2$ ($L_2$ = dppp) and $[(dppm\text{-}H)Pt(\mu\text{-}OH)]_2$ (eq 9). There is no reaction between $[(dppm\text{-}H)Pt(\mu\text{-}OH)]_2$ and $[L_2Pt(\mu\text{-}OH)]_2(BF_4)_2$ (L = $PMe_2Ph$). However, the anionic oxo complex $[(dppm\text{-}H)Pt(\mu\text{-}O)]_2Li_2$ readily deprotonates $[L_2Pt(\mu\text{-}OH)]_2(BF_4)_2$ ($L_2$ = dppp), yielding the dppp oxo complex (eq 10).

$$\underset{\mathbf{1}\ (L_2=\text{dppm})}{[(dppm)Pt(\mu\text{-}OH)]_2(BF_4)_2} + \underset{\mathbf{4}\ (L_2=\text{dppp})}{[L'_2Pt(\mu\text{-}O)]_2\cdot(LiBF_4)_2} \rightarrow \underset{\mathbf{1}\ (L_2=\text{dppp})}{[L'_2Pt(\mu\text{-}OH)]_2(BF_4)_2} + \underset{\mathbf{6}}{[(dppm\text{-}H)Pt(\mu\text{-}OH)]_2} + 2LiBF_4 \quad (9)$$

$$\underset{\mathbf{1}\ (L_2=\text{dppp})}{[L_2Pt(\mu\text{-}OH)]_2(BF_4)_2} + \underset{\mathbf{7}}{[(dppm\text{-}H)Pt(\mu\text{-}O)]_2Li_2} \rightarrow \underset{\mathbf{4}\ (L_2=\text{dppp})}{[L'_2Pt(\mu\text{-}O)]_2\cdot(LiBF_4)_2} + \underset{\mathbf{6}}{[(dppm\text{-}H)Pt(\mu\text{-}OH)]_2} + 2LiBF_4 \quad (10)$$

Combination of these results suggests a relative basicity order: $[(dppm\text{-}H)Pt(\mu\text{-}O)]_2Li_2$ > $[L_2Pt(\mu\text{-}O)]_2\cdot(LiBF_4)_2$ ($L_2$ = dppp, dppb, dppe) > $[L_2Pt(\mu\text{-}O)]_2\cdot(LiBF_4)_2$ (L = $PMe_2Ph$) > $[(dppm\text{-}H)Pt(\mu\text{-}OH)]_2$ > $[L_2Pt(\mu\text{-}O)]_2\cdot(LiBF_4)_2$ ($L_2$ = $Bu^t_2bpy$). This ordering is discussed further below.

## Discussion

**Hydroxo Complexes.** Initially, our interest in the hydroxo complexes $[L_2Pt(\mu\text{-}OH)]_2(BF_4)_2$ (**1**) was simply as precursors to the oxo complexes. However, the discovery that the $PMe_3$ hydroxo complex $[(PMe_3)_2Pt(\mu\text{-}OH)]_2(NO_3)_2$[10] showed an unusually short nonbonded hydroxo group O···O distance of 2.54 Å[14] attracted our attention and prompted us to examine the structure of some of our new hydroxo complexes. Of the three hydroxo complexes examined only the dppm complex has an unusual short O···O distance, and this is a remarkable 2.49 Å. The $PPh_3$ and dppb hydroxo complexes have distances (2.66 and 2.64 Å) close to those reported for the other Pt phosphine hydroxo complexes.[15,16] A comparison of the metrical parameters for Pt(II) phosphine hydroxo complexes is given in Table 5. While the dppm and $PMe_3$ complexes have the shortest O···O distances, they also have the longest Pt−Pt distances (3.270 and 3.261 Å versus 3.121−3.227 Å for the other complexes). We suspect that repulsive interactions between the Pt centers are responsible for the short O···O distances.[17,18] This is suggested by the smaller P−Pt−P angles and the higher basicity of dppm and $PMe_3$ of the two short O···O structures.

(13) (a) Camus, A.; Marsich, N.; Nardin, G.; Randaccio, L. *J. Organomet. Chem*. **1973**, *60*, C39. (b) Browning, J.; Bushnell, G. W.; Dixon, K. R. *J. Organomet. Chem*. **1980**, *198*, 11. (c) Bassett, J.-M.; Mandl, J. R.; Schmidbaur, H. *Chem. Ber*. **1980**, *113*, 1145. (d) Schmidbaur, H.; Mandl, J. R.; Bassett, J.-M.; Blaschke, G.; Zimmer-Gasser, B. *Chem. Ber*. **1981**, *114*, 433. (e) Brown, M. P.; Yavari, A.; Manojlovic-Muir, L.; Muir, K. W.; Moulding, R. P.; Seddon, K. R. *J. Organomet. Chem*. **1982**, *236*, C33. (f) Briant, C. E.; Hall, K. P.; Mingos, D. M. P. *J. Organomet. Chem*. **1982**, *229*, C5. (g) Manojlovic-Muir, L.; Muir, K. W. *Acta Crystallogr., C: Cryst. Struct. Commun.* **1986**, *42*, 272. (h) Meyer, E. M.; Gambarotta, S.; Floriani, C.; Chiesi-Villa, A.; Guastini, C. *Organometallics* **1989**, *8*, 1067. (i) Chebi, D. E.; Fanwick, P. E.; Rothwell, I. P. *Organometallics* **1990**, *9*, 2948. (j) Scherhag, F.; Kab, H.; Bright, T. A.; Malisch, W. *J. Organomet. Chem*. **1990**, *385*, C27. (k) Edema, J. J. H.; Meetsma, A.; van Bolhuis, F.; Gambarotta, S. *Inorg. Chem.* **1991**, *30*, 2056. (l) Gonzales, J. M. R.; Ruiz, J.; Granda, S. G.; Fayos, J. *Acta Crystallogr., C: Cryst. Struct. Commun.* **1991**, *47*, 706. (m) Okeya, S.; Shimomura, H.; Kushi, Y. *Chem. Lett*. **1992**, 2019.

(14) The sum of the van der Waals radii is 3.0 Å. Bondi, A. *J. Phys. Chem.* **1964**, *68*, 441.

(15) Bushnell, G. W. *Can. J. Chem*. **1978**, *56*, 1773.

(16) Longato, B; Pilloni, G; Valle, G.; Corain, B. *Inorg. Chem.* **1988**, *27*, 965−958.

(17) We thank Professor Odile Eisenstein for this suggestion.

**Table 5.** Comparative Distances (Å) and Angles (deg) for $[L_2Pt(\mu\text{-}OH)]_2^{2+}$ (L = a Phosphine)

| ligand | Pt−O | O···O | Pt···Pt | O−Pt−O | Pt−O−Pt | P1−Pt−P2 |
|---|---|---|---|---|---|---|
| $L_2$ = dppm | 2.06 | 2.49 | 3.270 | 74.6 | 105.4 | 73.6 |
| L = $PMe_3$[a] | 2.07 | 2.54 | 3.261 | 75.9 | 104.1 | 95.4 |
| $L_2$ = dppb | 2.08 | 2.64 | 3.215 | 78.8 | 101.2 | 101.2 |
| $L_2$ = dppf[b] | 2.10 | 2.68 | 3.227 | 79.4 | 100.6 | 98.1 |
| L = $PPh_3$ | 2.06 | 2.66 | 3.153 | 80.3 | 99.7 | 99.1 |
| L = $PEt_3$[c] | 2.13 | 2.72 | 3.121 | 79.4 | 94 | 97.7 |

[a] Reference 10. [b] Reference 16. [c] Reference 15.

**Table 6.** Comparative Distances (Å) and Angles (deg) for Oxo and Hydroxo Complexes

| ligand | Pt−O | O···O | Pt···Pt | O−Pt−O | Pt−O−Pt | P1−Pt−P2 |
|---|---|---|---|---|---|---|
| $L_2$ = dppm | | | | | | |
| hydroxo | 2.06 | 2.49 | 3.270 | 74.6 | 105.4 | 73.6 |
| $L_2$ = dppm-H | | | | | | |
| oxo | 2.05 | | 3.112 | 81.0 | 99.0 | 70.1 |
| L = $PPh_3$ | | | | | | |
| hydroxo | 2.06 | 2.66 | 3.153 | 80.3 | 99.7 | 99.1 |
| oxo | 2.03 | | 2.969 | 77.4 | 94.1 | 101.9 |

Both of these factors should enhance repulsive interactions between the two Pt centers, the small P−Pt−P angle leading to rehybridization[19] and the more basic phosphine putting more electron density on the Pt center. The dppm hydroxo complex does have the lowest $J_{PPt}$ values (3023 versus 3380 (dppp) to 3857 Hz (dppf)), indicating that this complex has the smallest amount of Pt s-character in the P−Pt bond.[20]

**Oxo Complexes.** The successful deprotonation of the Pt hydroxo complexes described above and in previous communications,[6] along with the previously reported deprotonations of $[(Cp^*Ir)_2(\mu\text{-}OH)_3]^+$ [21] and $[M_2(\mu\text{-}OH)(CO)_2(\mu\text{-}dppm)_2]^+$ (M = Rh, Ir),[3a] suggests that hydroxo complex deprotonation is a general route to late transition metal oxo complexes.[22] However, there are several alternative ways a "base" may react with a hydroxo complex that may lead to products other than the desired oxo complexes. Attack at the metal center is one.[23] Reduction of the metal center by electron transfer from the base is another. Even when deprotonation occurs, the site of deprotonation may not be the hydroxo group. This is clearly illustrated by the dppm complex where the dppm ligand is the initial site of deprotonation. The type of reaction can depend critically on the selection of the base. Of the four bases $LiN(SiMe_3)_2$, $LiNPr^i_2$, $LiBu^n$, and LiPh, only $LiN(SiMe_3)_2$ gives clean deprotonation of the $PPh_3$ hydroxo complex. With the other three, and especially with $LiBu^n$ and LiPh, significant amounts of $Ph_3PO$ are produced, suggesting that one or more of the alternative reaction pathways is being opened.

Spectroscopically, the most diagnostic feature of the formation of the Pt phosphine oxo complexes is the decrease in $J_{PPt}$ on deprotonation of the hydroxo ligand.[24] Donor properties of ligands trans to phosphines in square planar Pt(II) complexes are reflected in the P−Pt coupling constants. Stronger trans donors give a reduced coupling constant.[20] This is observed as the 300−500 Hz drop in the coupling constant on deprotonation of the hydroxo ligand to the strong donor oxo ligand. The coupling constant is sensitive enough to reveal interaction of the oxo group with Li ions. Thus, the coupling constant in $[L_2Pt(\mu\text{-}O)]_2\cdot LiBF_4$ (**2**) is 3286 Hz, while the coupling constant in $[L_2Pt(\mu\text{-}O)]_2$ (**3**), where there are no Li interactions, is over 100 Hz lower at 3180 Hz. This is consistent with a decrease in the donor ability of the oxo ligand resulting from the electron-withdrawing effect of the Li ion. The trimer **5** may be considered to result from the interaction of the oxo groups of $[L_2Pt(\mu\text{-}O)]_2$ with an $L_2Pt^{2+}$ fragment.[25] The $L_2Pt^{2+}$ fragment has a stronger electron-withdrawing effect than does $Li^+$, and the coupling constant increases from 3230 to 3480 Hz.

$^{17}O$ NMR shifts for early transition metal oxo complexes have been studied.[26] A correlation with multiple bonding has been observed and, in general, increasing multiple bonding gives larger shifts. Our $^{17}O$ NMR data is limited to the dppm complexes. The $^{17}O$ NMR shift of the cationic hydroxo complex $[L_2Pt(\mu\text{-}OH)]_2(BF_4)_2$ ($L_2$ = dppm) is 851 ppm. Deprotonation to the neutral dppm-H hydroxo complex [(dppm-H)Pt($\mu$-OH)]$_2$ (**6**) causes an increase to 877 ppm. Surprisingly, hydroxo group deprotonation with more $LiN(SiMe_3)_2$ to give the anionic oxo complex $[(dppm\text{-}H)Pt(\mu\text{-}O)]_2[Li(THF)_2]_2$ (**7**) does not cause a further shift (878 ppm). However, deprotonation with $NaN(SiMe_3)_2$ to give the sodium analog of **7** does result in a shift to 902 ppm. All of these shifts are in the range reported for early transition metal terminal oxo complexes (700−1200 ppm) with multiple metal−oxo bonding.[26] In comparison, the $^{17}O$ NMR chemical shift values reported for the late transition metal $\mu_3$-oxo complexes $[(LAu)_3(\mu\text{-}O)]^+$ (L = a phosphine) range between 19.7 and −36 ppm depending on the phosphine.[4c] That these are $\mu_3$-oxo complexes may explain why they are at much lower values than the $\mu_2$-oxo complexes reported here. Clearly, more $^{17}O$ NMR data is needed to establish trends for late transition metal systems.

The basicity of the Pt oxo complexes is measured by the p$K_a$ of the hydroxo complexes. Estimates of the p$K_a$ values could be made by evaluation of the equilibria described by eq 11 where BH represents an acid of known p$K_a$.[27] Such experiments have the same problems of solubility encountered in the competition experiments (eq 8, see above Results and below Discussion), only they are even more severe since equal solubility of BH and $[L_2Pt(\mu\text{-}OH)]_2(BF_4)_2$ would be very unlikely. We can, however, suggest an upper limit on the hydroxo complex p$K_a$ values. Since the hydroxo complexes are deprotonated by $LiN(SiMe_3)_2$ and $NaN(SiMe_3)_2$ (i.e., the equilibrium in eq 11 lies to the left even with the poor solubility of the hydroxo complexes favoring the right) the p$K_a$ values must be less than that of $HN(SiMe_3)_2$. The p$K_a$ of $HN(SiMe_3)_2$ is reported to be

(18) It is interesting to note that the recently reported structure of the $PMe_3$ Pd hydroxo complex, where M···M intereactions would be expected to be weaker, closely resembles the $PPh_3$ Pt complex and does not show a short O···O distance: Pieri, G.; Pasquali, M.; Leoni, P.; Englert, U. *J. Organomet. Chem.* **1995**, *419*, 27−30.

(19) Hofmann, P. In *Organometallics in Organic Synthesis*; de Meijiere, A., tom Dieck, H., Eds.; Springer: Berlin, 1987.

(20) (a) Hartley, F. R. *The Chemistry of Platinum and Palladium*; Appl. Sci. Publishers: Oxford, 1973. (b) Appleton, T. G.; Clark, H. C.; Manzer, L. E. *Coord. Chem. Rev.* **1973**, *10*, 335. (c) Shustorovich, E. M.; Porai-Koshits, M. A.; Buslaer, Yu. A. *Coord. Chem. Rev.* **1975**, *17*, 1. (d) Allen, F. H.; Pidcock, A. *J. Chem. Soc. A* **1968**, 2700. (e) Grim, S. O.; Wheatland, D. A. *Inorg. Nucl. Chem. Lett.* **1968**, *4*, 187.

(21) (a) McGhee, W. D.; Foo, T.; Hollander, F. J.; Bergman, R. G. *J. Am. Chem. Soc.* **1988**, *110*, 8543. (b) McGhee, W. D. Ph.D. Thesis, University of California, Berkeley, CA, 1987.

(22) Analogous deprotonations of amido complexes have also been reported. See: (a) ref 3. (b) Glueck, D. S.; Wu, J.; Hollander, F. J.; Bergman, R. G. *J. Am. Chem. Soc.* **1991**, *113*, 2041−2054. (c) Kolel-Veetil, M. K.; Ahmed, K. J. *Inorg. Chem.* **1994**, *33*, 4945−4949.

(23) We have observed such reactions with Au(I) hydroxo complexes. Yang, Y.; Sharp, P. R. Unpublished results.

(24) For the Rh and Ir A-frame hydroxo complexes, we found that the CO ligand IR bands are sensitive to deprotonation of the OH group.

(25) This is equivalent to viewing the oxo complex **3** as a bidentate ligand. The sulfido analog of **3** has been similarly viewed and was used to prepare a series of "coordination complexes": Gilmour, D.; Luke, M. A.; Mingos, D. M. P. *J. Chem. Soc., Dalton Trans.* **1987**, 335−340 and previous papers in a series.

(26) Klemperer, W. *Angew. Chem., Int. Ed. Engl.* **1978**, *17*, 246−254 and references cited therein.

(27) For a leading reference on the measurement of nonaqueous p$K_a$ values see: Bordwell, F. G. *Acc. Chem. Res.* **1988**, *21*, 456−463.

(28) Fraser, R. R.; Mansour, T. S.; Savard, S. *J. Org. Chem.* **1985**, *50*, 3232−33234.

25.8 in THF[28] and 26 in DMSO.[29] This sets an upper limit for the hydroxo complex p$K_a$ values of 25.

$$2BH + \underset{\mathbf{4}}{[L_2Pt(\mu\text{-}O)]_2\cdot(LiBF_4)_2} \rightleftarrows 2BLi + \underset{\mathbf{2}}{[L_2Pt(\mu\text{-}OH)]_2(BF_4)_2} \quad (11)$$

A lower limit is not possible to establish since protonation of the oxo complexes will always result in precipitation of the hydroxo complex. In addition, following reactions of the deprotonated acid may also complicate matters. As a result, deprotonation reactions by the oxo complexes are observed that would not be predicted on p$K_a$ arguments alone. For example, the p$K_a$ of $H_2O$ in non-hydrogen-bonding solvents is large and has been given a value of 31.2 in DMSO.[27] Assuming a similar value in THF and the upper limit hydroxo p$K_a$ of 25, reaction of the oxo complexes with $H_2O$ in THF would not be expected. Yet the oxo complexes do react. For L = $PPh_3$, the hydroxo complex is regenerated and precipitates from solution. LiOH must also be formed, and this may precipitate as well. These precipitations must favor the deprotonation of water. For the other phosphines the reaction with water is more complicated and appears to produce $L_2Pt(OH)_2$. In these cases, the formation of $L_2Pt(OH)_2$ increases the number of Pt−O bonds, which must also make the deprotonation of $H_2O$ favorable. Similarly, the $PPh_3$ oxo complex reacts with $PhNH_2$ (p$K_a$ = 30.6) to produce $L_2Pt(NHR)_2$ where Pt−N bond formation contributes favorably to the reaction.[30]

Although also complicated by precipitation reactions, an approximate relative basicity ranking of the oxo complexes is possible by the position of the equilibrium in eq 8. What is required is the assumption that the solubility of all the hydroxo complexes is the same. With this assumption, a ligand enhancement of the basicity in the order dppm-H > dppe ∼ dppp ∼ dppb > $PMe_2Ph$ > $Bu^t_2$bpy is found. For the most part, this ranking is reasonable. The dppp, dppb, and dppe ligands should have similar donor properties, so it is not surprising to find that the basicity of the oxo complexes of these ligands are all about the same. Similarly, the anionic dppm-H ligand should be a stronger donor, so the dppm-H oxo complex should be the most basic in the series. The low basicity of the $Bu^t_2$bpy oxo complex also seems reasonable given the higher electronegativity of nitrogen donor ligands and the possibility of $\pi$-back-bonding interactions with the bpy $\pi$-system. Both factors should decrease the electron density on the Pt centers, thus reducing the rise in energy of the oxo lone pair. Surprising, though, is the low basicity of the $PMe_2Ph$ complex. The $PMe_2$-Ph ligand is a stronger donor than the bis(diphenylphosphino) series of ligands. This anomaly can be explained if the solubility of the $PMe_2Ph$ hydroxo complex is greater than that of the other hydroxo complexes. This is not unreasonable with the reduction in the number of phenyl rings. A greater solubility would shift the equilibrium in eq 8 toward the $PMe_2Ph$ oxo complex, incorrectly indicating a lower basicity.

The instability of **4** (L = $PMe_2Ph$) and the formation of **5** are unique for the series of oxo complexes presented here. It is tempting to propose the expulsion of $Li_2O$ in the formation of **5** (eq 12). This appears to be too simple, as black precipitates and $Ph_3PO$ are also produced. Factors that might promote the decomposition for the $PMe_2Ph$ oxo complex are the low steric bulk and the high basicity of $PMe_2Ph$. The low steric demand would allow the more crowded geometry of **5**, and the high basicity should lead to lower acidity of the $L_2Pt^{2+}$ fragment, favoring a greater number of Pt−O interactions.

$$1.5\underset{\mathbf{4}\ (L = PMe_2Ph)}{[L_2Pt(\mu\text{-}O)]_2\cdot 2LiBF_4} \rightarrow \underset{\mathbf{5}}{[(L_2Pt)_3(\mu\text{-}O)_2](BF_4)_2} + Li_2O + LiBF_4 \quad (12)$$

**Structures.** The structural effects of deprotonation can be examined by a comparison of the structures of the hydroxo and oxo complexes. The best comparison is between the $PPh_3$ hydroxo and oxo complexes. While a major difference appears to be the edge-folded geometry of the oxo complex **2**, a folded geometry is also observed for the $PEt_3$ hydroxo complex.[14] Theoretical studies indicate a soft potential for folding in this type of dimer, and small perturbations can give bent or planar geometries.[31] Hydrogen bonding between the OH groups and the $BF_4$ ion was postulated to be the cause of the folded geometry in the $PEt_3$ hydroxo complex. The oxo−Li interactions may similarly be responsible for the fold in **2**. Although complicated by the deprotonation of the dppm ligand, oxo complex **7** may be planar because of the symmetric interactions of the oxo groups with the Li ions.

Rather remarkable is the close similarity of the Pt−O bond lengths of all of the hydroxo and oxo complexes. The averaged Pt−O distances within each complex range from 2.03 to 2.08 Å. The dppm-H (2.04(1) Å average) and the $PPh_3$ (2.03(1) Å average) oxo complexes are at the lower end of this range, suggesting that there is some shortening of the Pt−O distance on deprotonation. The hydroxo complexes and the $\mu_3$-oxo complex **5** distances are found at the long end (2.06, 2.06, 2.08, 2.08 Å). That **5** should be grouped with the hydroxo complexes is reasonable if one considers the replacement of two protons with an $L_2Pt^{2+}$ fragment. This grouping is consistent with the $J_{PPt}$ values, where low values are found for the $\mu_2$-oxo complexes but a higher value similar to those of the hydroxo complexes is found for the $\mu_3$-oxo complex **5**.

The bioxo-capped trinuclear structure of **5** is quite common for early transition metal systems. However, **5** is only the second bioxo-capped late transition metal complex.[32,33] The first is red $Ir_3(\mu_3\text{-}O)_2(\mu_2\text{-}I)(COD)_3$, isolated in 5% yield by chromatography of the reaction of $Ir_2I_2(\mu\text{-}I)_2(COD)_2$ with Ag(OAc).[34] The Ir complex is less symmetrical than **5** as the result of the bridging iodine atom and unequal Ir−Ir distances. Unfortunately, the details of the Ir structure were not reported, making further comparison of the structures impossible. Although not bioxo-capped, $\{(PPh_3)(CO)Rh\}_3(\mu_3\text{-}O)(\mu\text{-}OBu^t)$ and $[\{(binap)Rh\}_3(\mu_3\text{-}OH)_2]ClO_4$ have structures consisting of oxygen-ligand-bicapped triangular arrays of metal atoms.[35,36] The first

(29) Bordwell, F. G. as cited in: Grimm, D. T.; Bartmess, J. E. *J. Am. Chem. Soc.* **1992**, *114*, 1227. We thank J. Bartmess for this information.

(30) Li, J. J.; Li, W.; Sharp, P. R. To be published.

(31) ) Summerville, R. H.; Hoffmann, R. *J. Am. Chem. Soc.* **1976**, *98*, 7240.

(32) We have prepared several late transition metal heterometallic bioxo-capped trinuclear complexes from **3** or by displacement of $LiBF_4$ from $[(PPh_3)_2Pt(\mu\text{-}O)]_2\cdot LiBF_4$. These results will be reported in a future publication.

(33) Bisulfido-capped trinuclear late transition metal complexes are more common. For example, $[(L_2M)_3(\mu_3\text{-}S)_2]^{2+}$ (M = Ni, Pd, Pt), (a) Ghilardi, C. A.; Midollini, S.; Sacconi, L. *Inorg. Chim. Acta* **1978**, *31*, L431. (b) Matsumoto, K.; Saiga, N.; Tanaka, S.; Ooi, S. *J. Chem. Soc., Dalton Trans.* **1991**, 1265. (c) Werner, H.; Bertleff, W.; Schubert, U. *Inorg. Chim. Acta* **1980**, *43*, 199. (d) Bushnell, G. W.; Dixon, K. R.; Ono, R.; Pidcock, A. *Can. J. Chem.* **1984**, *62*, 696. (e) Pilkington, M. J.; Slawin, A. M. Z.; Williams, D. J.; Woollins, J. D. *J. Chem. Soc., Dalton Trans.* **1992**, 2425.

(34) Cotton, F. A.; Lahuerta, P.; Sanau, M.; Schwotzer, W. *J. Am. Chem. Soc.* **1985**, *107*, 8284−8285.

(35) Churchill, M. R.; Barkan, M. D.; Atwood, J. D.; Ziller, J. W. *Acta Crystallogr., Sect. C: Cryst. Struct. Commum.* **1990**, *46*, 2462−2465.

is perhaps the most closely related to **5** since one capping group is an oxo ligand. A comparison of its metrical parameters with **5** shows many similarities. The Rh−Rh distances are relatively short (2.938 Å average) as in **5** even though a metal−metal bond would not be expected. The metal−oxo distances and the angles around the oxo oxygen are also very similar with the Rh structure averaging 2.05 Å and 91.6°. In contrast, the Rh−O distances involving the $OBu^t$ group in $\{(PPh_3)(CO)Rh\}_3(\mu\text{-}O)(\mu_3\text{-}OBu^t)$ and the OH groups in $[\{binap)_2Rh\}_3(\mu_3\text{-}OH)_2]ClO_4$ are about 0.1 Å longer (2.154 and 2.151 Å), again suggesting that the metal−oxygen distances are reduced on going from an OH (or OR) group to an oxo group. Two independently isolated monocapped complexes differing only by the presence and absence of a proton on the capping oxygen atom are $[Pt_3(\mu_3\text{-}OH)(\mu\text{-}\eta^2\text{-}PPh_2O)_3(PPh_2Me)_3]PF_6$[37] and $[Pt_3(\mu_3\text{-}O)(\mu\text{-}\eta^2\text{-}PPh_2O)_3(PPh_2Me)_3](BF_4)_2$.[38] Unfortunately, no details of the oxo structure were reported, so only the Pt−O distances of the hydroxo complex are known. These average to 2.08 Å, essentially identical to those in **5**. Finally, there is the mixed valent complex $(DMSO)_4Pt_2(\mu_3\text{-}O)_2Pt_2Cl_2(DMSO)_2$.[39] In this complex, the oxo oxygens of a $(DMSO)_2Pt(\mu\text{-}O)_2Pt(DMSO)_2$ unit are bridged by the Pt(I) dimer (DMSO)ClPt−PtCl(DMSO) through Pt−O bonds. The Pt−O bonds are shorter than in **5** with Pt(II)−O bond distances of 2.03(1) Å and Pt(I)−O bond distances of 2.06(1) Å.

The X-ray data give us information on the structures of the isolated solids. Solution structures may be different. The behavior of the $PPh_3$ oxo complex suggests that this is so. The initial solid isolated from deprotonation of the hydroxo complex in THF is soluble in toluene and $Et_2O$ but only if not exposed to vacuum for extended periods. The toluene or $Et_2O$ solutions eventually precipitate crystals of **2** which are not soluble in $Et_2O$ or toluene. These observations suggest that the material isolated from THF, but not exposed to prolonged vacuum, has a somewhat different structure from that of **2**. While there are different shifts associated with these different solvent solutions, the $J_{PPt}$ values are constant and the same as the value ultimately observed in $CD_2Cl_2$ for isolated **2**. This suggests that if there are structural changes they do not noticeably affect the O−Pt interaction as reflected through the coupling constant. We believe that these observations are consistent with the initial formation of a product with THF molecules interacting with the Li ion. Loss of Li-coordinated THF (and perhaps $HN(SiMe_3)_2$) under vacuum or in $Et_2O$ or toluene produces **2** (eq 13). Both THF and $HN(SiMe_3)_2$ are detected in the $^1H$ NMR of the initially isolated solid. The solvent loss is apparently irreversible as the addition of THF (or $HN(SiMe_3)_2$) to **2** does not recover the toluene or $Et_2O$ solubility.

$$(L_2Pt)_2(\mu\text{-}O)_2Li(THF)_xBF_4 \rightarrow [L_2Pt(\mu\text{-}O)]_2LiBF_4 + xTHF \quad (13)$$
**2**

## Conclusions

Deprotonation of late transition metal hydroxo complexes has again proved to be an effective method for the synthesis of late transition metal oxo complexes yielding a series of Pt(II) dioxo dimers. As with the few other late transition metal oxo complexes prepared by this method, the Pt oxo complexes are strongly basic with estimated upper limit hydroxo complex $pK_a$ values of 25. A relative ranking of the hydroxo $pK_a$ values suggests a ligand enhancement of the basicity in the order dppm-H > dppe ∼ dppp ∼ dppb > $PMe_2Ph$ > $Bu^t_2bpy$. Structural data suggests a small decrease in the Pt−O bond distances on deprotonation of the hydroxo complexes to the oxo complexes.

## Experimental Section

**General Procedures**. Experiments were performed under a dinitrogen atmosphere in a Vacuum Atmospheres Corp. drybox or by Schlenk techniques unless otherwise indicated. Nonprotic solvents were dried under dinitrogen by recommended published techniques[40] and were stored under dinitrogen over 4 Å molecular sieves. NMR solvents were stored under dinitrogen over 4 Å molecular sieves. EtOH ("Anhydrous" 100%, McCormick Distilleries, MO), MeOH, and DMF were used as received except as noted. Alcohol/water mixtures were prepared on a volume basis. Silver tetrafluoroborate, silver trifluoroacetate, bis(diphenylphosphino)methane (dppm), bis(diphenylphosphino)ethane (dppe), bis(diphenylphosphino)propane (dppp), bis(diphenylphosphino)butane (dppb), dimethylphenylphosphine, 4-*tert*-butylpyridine, $LiN(SiMe_3)_2$, and $NaN(SiMe_3)_2$ were purchased from Aldrich Chemicals. $K_2PtCl_4$ was provided by Johnson Matthey as a loan or was prepared from Pt metal. $L_2PtCl_2$ ($L_2$ = dppm),[41] $[L_2Pt(\mu\text{-}OH)_2](BF_2)_2$ (L = $PPh_3$,[9a] $L_2$ = dppe[42]), and 4,4′-di-*tert*-butyl-2,2′-bipyridine[43] were synthesized according to literature procedures. $L_2PtCl_2$ ($L_2$ = dppp,[44] dppb) was prepared using the same procedure as for the $L_2$ = dppm complex. $L_2PtCl_2$ ($L_2$ = 4,4′-di-*tert*-butyl-2,2′-bipyridine) was prepared using the same procedure as for the $L_2$ = bpy complex.[9b] $^1H$ NMR spectra were recorded on a Nicolet NT-300WB spectrometer or a Bruker AMX-500 spectrometer referenced to TMS or to protic impurities referenced back to TMS. $^{31}P$ NMR spectra were obtained on a Jeol FX 90Q or a Nicolet NT 300WB spectrometer with an external $H_3PO_4$ reference. $^{19}F$ NMR spectra were obtained on a Bruker AMX-250 spectrometer operating at 235 MHz with an external $CF_3C_6H_5$ reference. $^{17}O$ NMR spectra were obtained on a Bruker AMX-500 spectrometer operating at 67.8 MHz with an external water reference. All NMR shifts are in ppm with negative shifts upfield from the reference. Infrared spectra were recorded on a Nicolet 20 DXB FTIR spectrometer using NaCl plates. All spectra were recorded at ambient temperatures unless otherwise indicated. Microanalyses (inert atmosphere) were performed by Desert Analytics or Oneida Research Services, Inc.

**Hydroxo Complexes. $[L_2Pt(\mu\text{-}OH)]_2(BF_4)_2$ (1).** The successful synthesis of these complexes depends on the solvent and the amount of water present in the solvent. When alcohol solvents are used, inadequate amounts of water in the solvent result in the formation of mixtures of the desired hydroxo complexes and what NMR data suggests are the alkoxo analogs. Excessive water gives black precipitates. The complexes are not air sensitive, but many are hygroscopic.

**$L_2$ = dppm.** A solution of $AgBF_4$ (0.390 g, 2.00 mmol) in 10 mL of EtOH was added dropwise to a suspension of $L_2PtCl_2$ (0.650 g, 1.00 mmol) in EtOH (40 mL). The reaction mixture was stirred for 3 h and filtered. The isolated solid was washed with EtOH (20 mL), dried in vacuo for 4 h, and then extracted with DMF (5 mL). Addition of $Et_2O$ (150 mL) to the filtered DMF solution gave a white precipitate, which was recovered by filtration and dried in vacuo. Yield: 0.725 g (96%). Crystals for analysis and X-ray work were grown from DMF/$Et_2O$. Anal. Calcd (found) for $Pt_2P_4N_2O_4B_2F_8C_{56}H_{60}$ $\{[(dppm)Pt(\mu\text{-}OH)]_2(BF_4)_2\cdot 2DMF\}$: C, 44.46 (44.24, 44.10); H, 4.00 (3.85, 3.92); N, 1.85 (1.83, 1.83). The presence of DMF was confirmed by $^1H$ NMR

(36) Yamagata, T.; Tani, K.; Tatsuno, Y.; Saito, T. *J. Chem. Soc., Chem. Commun.* **1988**, 466.
(37) Alcock, N. W.; Bergamini, P.; Gomes-Carniero, T. M.; Jackson, R. D.; Nicholls, J.; Orpen, A. G.; Pringle, P. G.; Sostero, S.; Traverso, O. *J. Chem. Soc., Chem. Commun.* **1990**, 980−982.
(38) Lin, I. J. B.; Lai, J. S.; Liu, L-.K.; Wen, Y. S. *J. Organomet. Chem.* **1990**, *399*, 361−364.
(39) Betz, P.; Bino, A. *J. Am. Chem. Soc.* **1988**, *110*, 602−603.
(40) Burfield, D. R.; Lee, K. -H.; Smithers, R. H. *J. Org. Chem.* **1977,** *42*, 3060.
(41) Brown, M. P.; Puddephatt, R. J.; Rashidi, M.; Seddon, K. R. *J. Chem. Soc., Dalton Trans.* **1977**, 951−955.
(42) Scarcia, V.; Furlani, A.; Longato, B.; Corain, B. *Inorg. Chim. Acta* **1988**, *153*, 67−70.
(43) Hadda, T. B.; Le Bozec, H. *Polyhedron* **1988**, *7*, 575−577.
(44) An alternative preparation is given: Appleton, T. G.; Bennett, M. A.; Tomkins, I. B. *J. Chem. Soc., Dalton Trans.* **1976**, 439.

spectroscopy and the X-ray crystal structure determination. IR (mineral oil): 3200 (m, $\nu_{OH}$) $cm^{-1}$. $^1H$ NMR (500 MHz, DMSO-$d_6$): 7.2−7.8 (m, 40H, phenyl), 5.20 (t, $J_{PH}$ = 25 Hz, 4H, $CH_2$), 6.50 (s, 2, OH). $^{31}P\{^1H\}$ NMR (121 MHz, DMSO): −64 ($J_{PPt}$ = 3023 Hz). $^{17}O\{^1H\}$ NMR (THF); 851 ($\nu_{1/2}$ = 42 Hz) ppm.

The $^{17}O$-enriched sample was prepared as follows. A solution of $AgBF_4$ (0.078 g, 0.400 mmol) in 5 mL of EtOH was added dropwise to a suspension of (dppm)$PtCl_2$ (0.130 g, 0.200 mmol) in 10 mL of EtOH. The reaction mixture was stirred for 3 h and filtered. The precipitate was washed with EtOH (5 mL) and dried in vacuo. DMF (3 mL, dried over 4 Å molecular sieves) and $H_2{}^{17}O$ (40%, 0.027 g, 0.150 mmol) were added to the solid. After 5 min of stirring the mixture was filtered, and $Et_2O$ (40 mL) was added to the filtrate. The resulting white precipitate was recovered by filtration and dried in vacuo. Yield: 0.136 g (90%).

**$L_2$ = dppp.** A solution of $AgBF_4$ (0.780 g, 4.00 mmol) in 20 mL of 90% MeOH was added to a suspension of $L_2PtCl_2$ (1.356 g, 2.00 mmol) in 100 mL of 90% MeOH. The reaction mixture was stirred for 2 h and filtered. The filtrate was concentrated in vacuo to ca. 15 mL. The resulting white microcrystalline precipitate was recovered by filtration, washed with a small amount of cold MeOH, and dried in vacuo. Yield: 0.996 g (70%). Anal. Calcd (found) for $C_{54}H_{54}B_2F_8O_2P_4Pt_2$: C, 45.58 (44.65); H, 3.82 (3.62). With 1.5$H_2O$: C 44.74; H 3.96. IR (mineral oil): 3550 (m, $\nu_{OH}$) $cm^{-1}$. $^1H$ NMR (300 MHz, DMSO-$d_6$): 7.3−7.8 (m, 40H, phenyl), 2.9 (broad, 4H, $PCH_2CH_2CH_2P$), 1.88 (s, 2H, OH), 1.7 (broad, 8H, $PCH_2CH_2CH_2CH_2P$). $^{31}P\{^1H\}$ NMR (121 MHz, DMSO): −9.8 ($J_{PPt}$ = 3380 Hz).

The analogous trifluoroacetate salt was prepared as follows. A solution of $CF_3CO_2Ag$ (0.470 g, 2.00 mmol) in 20 mL of MeOH (dried over 4 Å molecular sieves) was added to a suspension of $L_2PtCl_2$ (0.678 g, 1.00 mmol) in 100 mL of MeOH (dried over 4 Å molecular sieves). The mixture was stirred for 2 h and then filtered. The filtrate was concentrated in vacuo to ca. 15 mL, and the resulting white solid was removed by filtration, washed with a small amount of cold MeOH (dried over 4 Å molecular sieves), and dried in vacuo. The solid (0.690 g, presumably $L_2Pt(CF_3CO_2)_2$) was redissolved in MeOH (100 mL), and a solution of NaOH (0.032 g, 0.80 mmol) in 10 mL of $H_2O$ was added. The mixture was stirred for 0.5 h and filtered. The filtrate was concentrated in vacuo to ca. 15 mL, and the resulting white solid was removed by filtration, washed with a small amount of cold MeOH, and dried in vacuo. Yield: 0.645 g (75%). Failure to remove the Ag salts by this two-step procedure prior to the addition of the NaOH resulted in the formation of black intractable mixtures. NMR data are the same as for the $BF_4$ salt.

**$L_2$ = dppb.** A solution of $AgBF_4$ (0.780 g, 4.00 mmol) in 20 mL of 95% MeOH was added to a suspension of $L_2PtCl_2$ (1.356 g, 2.00 mmol) in 95% MeOH (100 mL). The reaction mixture was stirred for 1 h and then filtered. The filtrate was concentrated in vacuo to ca. 10 mL. The resulting white microcrystalline precipitate was recovered by filtration and washed with a small amount of cold MeOH. Yield: 1.088 g (75%). Single crystals suitable for X-ray diffraction were obtained from MeOH/$Et_2O$ and were subject to decomposition by solvent loss. Anal. Calcd (found) for $C_{56}H_{58}B_2F_8O_2P_4Pt_2$: C, 46.36 (45.94); H, 4.01 (3.84). IR (mineral oil): 3550 (m, $\nu_{OH}$) $cm^{-1}$. $^1H$ NMR (300 MHz, DMSO-$d_6$): 7.3−7.8 (m, 40H, phenyl), 2.8 (broad, 8H, $PCH_2CH_2CH_2CH_2P$), 1.8 (broad, 8H, $PCH_2CH_2CH_2CH_2P$), 1.32 (s, 2H, OH). $^{31}P\{^1H\}$ NMR (121 MHz, DMSO): −5.0 ($J_{PPt}$ = 3500 Hz).

**L = $PMe_2Ph$.** A solution of $AgBF_4$ (0.390 g, 2.00 mmol) in 90% EtOH (5 mL) was added to a suspension of $L_2PtCl_2$ (0.542 g, 1.00 mmol) in 25 mL of 90% EtOH. The reaction mixture was stirred for 40 min and then filtered. The filtrate was concentrated in vacuo to ca. 10 mL. Addition of 120 mL of $Et_2O$ gave a white precipitate, which was recovered by filtration and dried in vacuo. The pure product can be recrystallized from EtOH/$Et_2O$. Yield: 0.408 g (71%). IR (mineral oil): 3450 (m, $\nu_{OH}$) $cm^{-1}$. $^1H$ NMR (300 MHz, DMSO-$d_6$): 7.8−8.2 (m, 20H, phenyl), 4.02 (s, 2H, OH), 1.48 (d, $J_{PH}$ = 14 Hz, 24H, $PCH_3$). $^{31}P\{^1H\}$ NMR (121 MHz, DMSO): −15.7 ($J_{PPt}$ = 3460 Hz).

**$L_2$ = 4,4′-di-*tert*-butyl-2,2′-bipyridine.** The $BF_4$ salt was prepared as follows. A mixture of (0.534 g, 1.00 mmol) of $L_2PtCl_2$ and (0.390 g, 2.00 mmol) of $AgBF_4$ in EtOH (100 mL) was heated to 60 °C with stirring. After 4 h, the light yellow product was recovered by filtration and dried in vacuo. Yield: 0.325 g (60%). NMR data were the same as for the nitrate salt.

The analogous nitrate salt was prepared as follows. A mixture of (0.534 g, 1.00 mmol) of $L_2PtCl_2$ and (0.348 g, 2.00 mmol) of $AgNO_3$ in water (60 mL) was heated to 80 °C with stirring. After 24 h the mixture was filtered. The solid was extracted with EtOH (250 mL), and the light yellow product was isolated by removing the volatiles in vacuo. Yield: 0.423 g (70%). Anal. Calcd (Found) for $C_{36}H_{50}N_4O_2B_2F_8Pt_2$: C, 39.85 (39.80); H, 4.61 (4.45); N, 7.75 (7.54). IR (mineral oil): 3550 (m, $\nu_{OH}$) $cm^{-1}$. $^1H$ NMR (300 MHz, DMSO-$d_6$): 8.80 (d, $J_{HH}$ = 7 Hz, 4H, 5/6-H-ring), 7.92 (s, 4H, 3-H-ring), 7.65 (d, $J_{HH}$ = 7 Hz, 4H, 5/6-H-ring), 5.95 (s, 2H, OH), 1.38 (s, 36H, $Bu^t$).

**Oxo Complexes.** The oxo complexes are highly sensitive to moisture. Solvents must be dry, and all operations must be conducted in an inert atmosphere. All, except the $Bu^t_2$-bpy, react with $CH_2Cl_2$, and all react with $CHCl_3$ and protic solvents.

**$[L_2Pt(\mu\text{-}O)]_2\cdot(LiBF_4)$ (2) (L = $PPh_3$).** $[L_2Pt(\mu\text{-}OH)]_2(BF_4)_2$ (100 mg, 0.0607 mmol) was suspended in 2 mL of THF. A 5 mL THF solution of $LiN(SiMe_3)_2$ (41 mg, 0.245 mmol) was added dropwise with stirring. The reaction mixture turned into a homogeneous pale yellow solution in ca. 0.5 h ($^{31}P\{^1H\}$ NMR: 7.8 ($J_{PPt}$ = 3286 Hz)). All volatiles were removed in vacuo. The crystalline residue was extracted with 4 mL of toluene ($^{31}P\{^1H\}$ NMR: 12.7 ($J_{PPt}$ = 3286 Hz)). Two milliliters of ether was added to the toluene extract. The resulting white solid was collected by filtration, washed with ether, and dried in vacuo. Yield: 84 mg (88%). $^{31}P\{^1H\}$ NMR (121 MHz, $CH_2Cl_2$): 11.4 ($J_{PPt}$ = 3286 Hz). $^{19}F$ NMR (toluene): −2.09 (s). IR (mineral oil): 1054 (s, $\upsilon_{BF}$) $cm^{-1}$.

Single crystals suitable for X-ray diffraction were grown from the toluene extract by cooling to −30 °C overnight. Crystals for analysis were obtained by extraction of the THF reaction residue with $Et_2O$ instead of toluene. The $Et_2O$ extract deposited crystals overnight. Anal. Calcd (Found) for $C_{72}H_{60}BF_4LiO_2P_4Pt_2\cdot 2Et_2O$: C, 56.08 (56.17); H, 4.71 (4.93); N, 0.00 (0.40). The presence of $Et_2O$ was confirmed by $^1H$ NMR spectroscopy.

**$[L_2Pt(\mu\text{-}O)]_2$ (3) (L = $PPh_3$).** A THF (1 mL) solution of $NaN(SiMe_3)_2$ (30 mg, 0.166 mmol) was added to a stirred suspension of $[L_2Pt(\mu\text{-}OH)]_2(BF_4)_2$ (100 mg, 0.067 mmol) in 2 mL of THF. The mixture was stirred for about an hour when almost everything was dissolved ($^{31}P\{^1H\}$ NMR: 8.4 ($J_{PPt}$ = 3180 Hz)). The mixture was then filtered, and the volatile materials were removed in vacuo. The residue was extracted with 2 mL of toluene ($^{31}P\{^1H\}$ NMR: 10.7 ($J_{PPt}$ = 3180 Hz)) and $Et_2O$ (2 mL) was added to the extract. The resulting white solid product was collected by filtration, washed with $Et_2O$, and dried in vacuo. Yield: 64 mg (66%). $^{31}P\{^1H\}$ NMR (121 MHz, $CH_2Cl_2$): 10.3 ($J_{PPt}$ = 3180 Hz).

**$[L_2Pt(\mu\text{-}O)]_2\cdot(LiBF_4)_2$ (4). $L_2$ = dppe.** A solution of $LiN(SiMe_3)_2$ (0.071g, 0.400 mmol) in 2 mL of THF was added very slowly to a suspension of $[L_2Pt(\mu\text{-}OH)]_2(BF_4)_2$ (0.278 g, 0.200 mmol) in 10 mL of THF at −30 °C. The reaction mixture was stirred for 10 min and filtered. The filtrate was concentrated in vacuo to ca. 2 mL, and hexane was added. The resulting white precipitate was recovered by filtration, washed with cold THF and $Et_2O$, and dried in vacuo. Yield: 0.179 g (72%). $^1H$ NMR (300 MHz, THF-$d_8$): 6.8−8.3 (m, 40H, phenyl), 2.4 (broad, 8H, $PCH_2CH_2P$). $^{31}P\{^1H\}$ NMR (36 MHz, THF): 23.0 ($J_{PPt}$ = 3120 Hz). $^{19}F$ NMR (THF): 112.1 (s, $BF_4$). Integration of the $BF_4$ signal versus added $CF_3SO_3Li$ indicated the presence of two $BF_4$ ions.

**$L_2$ = dppp.** A solution of $LiN(SiMe_3)_2$ (0.071 g, 0.400 mmol) in 2 mL of THF was added dropwise to a stirred suspension of $[L_2Pt(\mu\text{-}OH)]_2(BF_4)_2$ (0.284 g, 0.200 mmol) in 10 mL of THF. The reaction mixture was stirred for 10 min and then filtered. The filtrate was concentrated in vacuo to ca. 2 mL. Hexane was added, and the mixture was stored at −30 °C for 2 h. The precipitated light yellow product was recovered by filtration, washed with cold THF and $Et_2O$, and dried in vacuo. Yield: 0.169 g (68%).

The trifluoroacetate salt was similarly prepared from $[L_2Pt(\mu\text{-}OH)]_2(CF_3CO_2)_2$. Data for the trifluoroacetate salt are reported. Anal. Calcd (found) for $C_{58}H_{52}F_6Li_2O_6P_4Pt_2$: C, 46.85 (46.80); H, 3.52 (3.56). $^1H$ NMR (300 MHz, THF-$d_8$): 7.1−7.8 (m, 40H, phenyl), 2.7 (broad, 4H, $PCH_2CH_2H_2P$), 1.9 (broad, 8H, $PCH_2CH_2CH_2P$). $^{31}P\{^1H\}$ NMR (121 MHz, THF): −16.0 ($J_{PPt}$ = 3040 Hz). $^{19}F$ NMR (THF): 32.5 (s, $CF_3$-

$SO_3$). Integration of the trifluoroacetate signal versus added $LiBF_4$ confirmed the presence of two trifluoroacetate ions.

**$L_2$ = dppb**. A solution of $LiN(SiMe_3)_2$ (0.071 g, 0.400 mmol) in 2 mL of THF was slowly added to a suspension of $[L_2Pt(\mu\text{-}OH)]_2(BF_4)_2$ (0.290 g, 0.200 mmol) in 10 mL of THF. The reaction mixture was stirred for 20 min and filtered. The filtrate was slowly concentrated in vacuo to ca. 2 mL. The resulting yellow microcrystalline product was recovered by filtration, washed with cold THF, and dried in vacuo. Yield: 0.200 g (78%). $^1$H NMR (300 MHz, THF-$d_8$): 7.2−7.6 (m, 40H, phenyl), 2.5 (broad, 8H, $PCH_2CH_2CH_2CH_2P$), 1.8 (broad, 8H, $PCH_2CH_2CH_2CH_2P$). $^{31}P\{^1H\}$ NMR (121 MHz, THF): −1.6 ($J_{PPt}$ = 3180 Hz). $^{19}$F NMR (THF): 112.1 (s, $BF_4$). Integration of the $BF_4$ signal versus added $CF_3SO_3Li$ indicated the presence of two $BF_4$ ions.

**$L_2$ = 4,4′-Di-*tert*-butyl-2,2′-bipyridine.** A solution of $LiN(SiMe_3)_2$ (0.071 g, 0.400 mmol) in 2 mL of THF was added dropwise to a suspension of $[L_2Pt(\mu\text{-}OH)]_2(BF_4)_2$ (0.217 g, 0.200 mmol) in 10 mL of THF. The initial yellow solution became orange and finally red. The reaction mixture was stirred a total of 10 min and then filtered. The filtrate was slowly concentrated in vacuo to ca. 2 mL, and then $Et_2O$ (15 mL) was added to precipitate a red solid. The red product was collected by filtration and dried in vacuo. Yield: 0.173 g (78%). Anal. Calcd (found) for $C_{36}H_{48}Li_2N_4O_2B_2F_8Pt_2$: C, 37.72 (37.87); H, 4.22 (4.50); N, 4.89 (4.97). $^1$H NMR (300 MHz, $CD_2Cl_2$): 8.78 (d, $J_{HH}$ = 8.5 Hz, 4H, 5/6-ring-H), 7.95 (s, 4H, 3-ring-H), 7.71 (d, $J_{HH}$ = 8.5 Hz, 4H, 5/6-ring-H), 1.39 (s, 36H, Bu$^t$).

**L = $PMe_2Ph$.** A solution of $LiN(SiMe_3)_2$ (0.043 g, 0.250 mmol) in 1 mL of THF was added slowly to a suspension of $[L_2Pt(\mu\text{-}OH)]_2(BF_4)_2$ (0.144 g, 0.125 mmol) in 4 mL of THF at −30 °C. The reaction mixture was stirred for 10 min and filtered. The filtrate was concentrated in vacuo to ca. 1.5 mL. Hexane was added, and the mixture was stored at −30 °C for 4 h. The resulting light yellow solid was recovered by filtration, washed with cold THF, and dried in vacuo. Yield: 0.098 g (80%). $^1$H NMR (300 MHz, THF-$d_8$): 7.7−8.3 (m, 20H, Ph), 1.50 (d, $J_{HP}$ = 14 Hz, 24H, Me). $^{31}$P NMR (121 MHz, THF): −17.5 ($J_{PPt}$ = 3230 Hz). $^{19}$F NMR (THF): 112.1 (s, $BF_4$). Integration of the $BF_4$ signal versus added $CF_3SO_3Li$ indicated the presence of two $BF_4$ ions.

**$[(L_2Pt)_3(\mu\text{-}O)_2](BF_4)_2$ (5) (L = $PMe_2Ph$).** To a suspension of $[L_2Pt(\mu\text{-}OH)]_2(BF_4)_2$ (0.144 g, 0.125 mmol) in 4 mL of THF, a solution of $LiN(SiMe_3)_2$ (0.043 g, 0.250 mmol) in 1 mL of THF was added slowly at room temperature. The reaction mixture was stirred for 3 h and filtered. The filtrate was concentrated in vacuo to ca. 1.5 mL and then stored under −30 °C. After 1 day, crystals had formed. These were recovered by filtration and dried in vacuo. Yield: 0.088 g (70%). $^1$H NMR (300 MHz, $CD_2Cl_2$): 7.6−8.2 (m, 20H, Ph), 1.50 (d, $J_{HP}$ = 14 Hz, 24H, Me). $^{31}$P NMR (121 MHz, THF): 19.6 ($J_{PPt}$ = 3480 Hz).

**$[(dppm\text{-}H)Pt(\mu\text{-}OH)]_2$ (6).** A solution of $LiN(SiMe_3)_2$ (0.088 g, 0.500 mmol) in 2 mL of THF was added dropwise to a suspension of $[L_2Pt(\mu\text{-}OH)]_2(BF_4)_2$ (0.378 g, 0.250 mmol) in THF (10 mL). The reaction mixture immediately turned into a homogeneous yellow solution. The solution was concentrated in vacuo to ca. 1.5 mL, and the filtrate gave a yellow precipitate, which was washed by 1 mL of THF and dried in vacuo. Yield: 0.208 g (70%). Anal. Calcd (found) for $C_{50}H_{44}O_2P_4Pt_2$: C, 50.42 (50.12); H, 3.73 (3.75). $^1$H NMR (300 MHz, THF-$d_8$): 7.0−7.8 (m, 40H, Ph), 3.95 (s, 2H, OH), −0.34 (s, 2H, PCHP). $^{31}P\{^1H\}$ NMR (121 MHz, THF): −69.0 ($J_{PPt}$ = 2830 Hz). $^{17}O\{^1H\}$ NMR (THF) 877 ($\nu_{1/2}$ = 29 Hz) ppm. The $^{17}$O-enriched sample was prepared by deprotonation of $^{17}$O-enriched $[L_2Pt(\mu\text{-}OH)]_2(BF_4)_2$.

**$[(dppm\text{-}H)Pt(\mu\text{-}O)_2](Li)_2\cdot 4THF$ (7).** A solution of $LiN(SiMe_3)_2$ (0.071 g, 0.400 mmol) in THF (1 mL) was added dropwise to a yellow suspension of $[(dppm\text{-}H)Pt(\mu\text{-}OH)]_2$ (0.218 g, 0.200 mmol) in THF (3 mL) at −30 °C. The reaction mixture immediately turned into a homogeneous yellow solution. The solution was concentrated in vacuo to ca. 2 mL. Storage of the concentrated solution at −30 °C gave yellow crystals, which were isolated by filtration and dried in vacuo. Yield: 0.208 g (95%). $^{31}P\{^1H\}$ NMR (121 MHz, THF): −54.4 ($J_{PPt}$ = 2430 Hz). $^{17}O\{^1H\}$ NMR (THF): 878 ($\nu_{1/2}$ = 22 Hz) ppm. The $^{17}$O-enriched complex for NMR was prepared from enriched $[(dppm\text{-}H)Pt(\mu\text{-}OH)]_2$. The enriched sodium analog, $[(dppm\text{-}H)Pt(\mu\text{-}O)_2](Na)_2$, was similarly prepared by using $NaN(SiMe_3)_2$ in place of $LiN(SiMe_3)_2$ and gave the following spectral data. $^{31}$P NMR (121 MHz, THF): −54.4 ($J_{PPt}$ = 2360 Hz). $^{17}O\{^1H\}$ NMR (THF): 920 ($\nu_{1/2}$ = 16 Hz) ppm.

**Crystal Structure Analyses**. Crystal data, reflection collection and processing parameters, and solution and refinement data are summarized in Table 1 and fully displayed in the supporting information. Crystals were grown as described above. Structures were done at subambient temperatures when the samples were found to be sensitive to air exposure. These sensitive crystals were mounted by pipeting a sample of crystals and mother liquor into a pool of heavy oil. A crystal was selected and removed from the oil with a glass fiber. With the oil-covered crystal adhering to the end of the glass fiber, the sample was transferred to an $N_2$ cold stream on the diffractometer. Structures done at ambient temperatures had samples mounted on the end of a glass fiber with epoxy.

**Acknowledgment.** We thank the Division of Chemical Sciences, Office of Basic Energy Sciences, Office of Energy Research, U.S. Department of Energy (DE-FG02-88ER13880) for support of this work and Johnson Matthey for loans of precious metal salts. Grants from the National Science Foundation provided a portion of the funds for the purchase of the X-ray (NSF-CHE-9011804) and NMR (Grants 8908304 and 9221835) equipment.

**Supporting Information Available:** Details of the X-ray structures, including tables of fractional coordinates, thermal parameters, and complete bond distances and angles (33 pages). Ordering information is given on any current masthead page.

IC950593S